International Journal of Microwave and Wireless Technologies

cambridge.org/mrf

Design of TE-polarized resonant Bessel-beam launchers for wireless power transfer links in the radiative near-field region

Edoardo Negri[1], Francesca Benassi[2], Walter Fuscaldo[3], Diego Masotti[2], Paolo Burghignoli[1], Alessandra Costanzo[2] and Alessandro Galli[1]

[1]Department of Information Engineering, Electronics and Telecommunications (DIET), Sapienza Univeristy of Rome, Rome, Italy; [2]Department of Electrical, Electronic and Information Engineering "Guglielmo Marconi" (DEI), University of Bologna, Bologna, Italy and [3]Istituto per la Microelettronica e Microsistemi (IMM), Consiglio Nazionale delle Ricerche, Rome, Italy

Research Paper

Cite this article: Negri E, Benassi F, Fuscaldo W, Masotti D, Burghignoli P, Costanzo A, Galli A (2024) Design of TE-polarized resonant Bessel-beam launchers for wireless power transfer links in the radiative near-field region. *International Journal of Microwave and Wireless Technologies*, 1–10. https://doi.org/10.1017/S1759078723001538

Received 15 June 2023
Revised 29 November 2023
Accepted 1 December 2023

Keywords:
Bessel beams; Fabry–Perot cavities; leaky waves; metasurfaces; wireless power transfer

Corresponding author: Edoardo Negri; Email: edoardo.negri@uniroma1.it

Abstract

Resonant Bessel-beam launchers (BBLs) are radiating devices constituted by a cylindrical metallic cavity with a partially reflecting sheet (PRS) on top. Millimeter-wave resonant BBLs typically exhibit transverse magnetic (TM) polarization due to the use of coaxial probes as feeders and homogenized metasurfaces as PRS. Launchers showing either a *purely* transverse electric (TE) or a *hybrid* (quasi-TE) polarization have recently been proposed for realizing wireless power transfer (WPT) links in the radiative near-field region at millimeter waves. The former are obtained by means of a radial slot array as a feeder and a homogenized metasurface as a PRS. The latter are obtained by using a loop antenna as a feeder and an annular strip grating in the homogenization limit as radiating aperture. In this work, based on an original semi-analytical model, such a metasurface is demonstrated to show a dichroic behavior. This interpretation explains the improvement in terms of polarization purity with respect to more nondichroic conventional homogenized metasurfaces. The behavior of the annular strip grating under a pure TM polarization is tested with a coaxial feeder, whereas its behavior under a pure TE polarization is tested by means of the radial slot array feeder. Results confirm the validity of the proposed analysis, which is finally exploited to evaluate the WPT performance.

Introduction

An earlier version of this paper was presented at the 52nd European Microwave Conference and was published in its Proceedings [1]. In paper [1], the authors have shown the possibility to exploit a *purely* transverse electric (TE-) Bessel beam in a wireless power transfer (WPT) scenario. In this work, a thorough analysis of the devices discussed in paper [1] is presented both from a theoretical and a practical viewpoint.

Bessel beams are monochromatic solutions of Helmholtz equation in a cylindrical reference frame [2] with focusing, limited-diffraction, and self-healing properties (i.e., the capability to reconstruct themselves after an obstacle placed along the beam axis) [3–6]; such features are particularly attractive for WPT applications in the microwave and/or millimeter-wave range (see, e.g., [7–13]).

Many kinds of Bessel-beam launchers (BBLs), i.e., devices able to generate a Bessel beam, have been proposed in the microwave and millimeter-wave range [14]. Two families of launchers can be distinguished in terms of their frequency behavior: wideband BBLs [15–18] feature a large bandwidth at the expense of an electrically large aperture size, whereas resonant BBLs [19–21] are compact in size but typically feature a narrow frequency band.

In a WPT scenario, the bandwidth is of minor concern, whereas a compact size might play a crucial role as, e.g., in WPT for wearable and implantable devices [22]. As a result, resonant BBLs are preferable due to their limited transverse size. Resonant BBLs are typically constituted by a metallic cavity whose upper plate is replaced by a partially reflecting sheet (PRS), which is often a homogenized metasurface. Dipole-like sources are often considered for exciting such cavities [23].

As already discussed in paper [1], in most of the reported experiments on BB launchers (see, e.g., [15, 19, 24]), these are fed with coaxial probes, which are ideally equivalent to vertical electrical dipoles (VEDs), and thus excite transverse magnetic (TM) polarized Bessel beams. From a theoretical viewpoint, a TE-polarized Bessel beam has to be excited by means of a vertical magnetic dipole (VMD). The latter, however, does not have a simple physical implementation. As shown in papers [25, 26], the VMD could be implemented by loop antennas or coils but the feeding point breaks the azimuthal symmetry, thus generating undesired TM-field components [8].

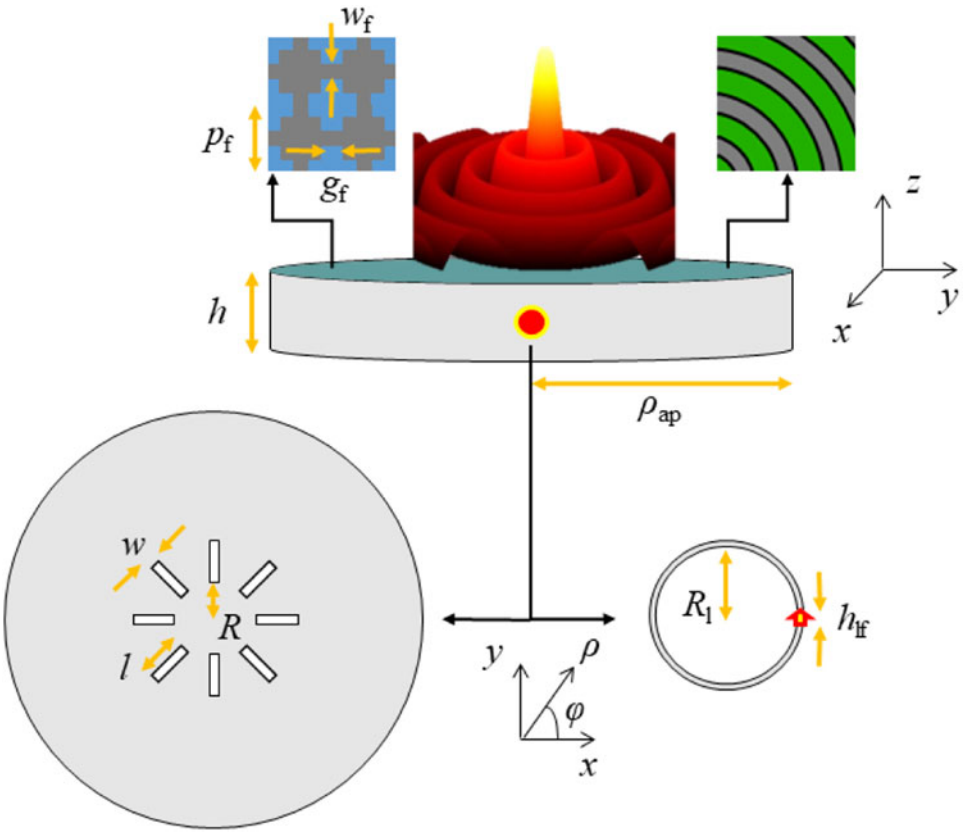

Figure 1. Pictorial representation of a TE-polarized resonant BBL and of its H_z field distribution through a three-dimensional colormap. The BBL consists of a metallic cavity of height h and radius ρ_{ap} with a PRS (reported through an aqua green color) on top. TE-polarized resonant BBLs can be excited by means of either loop-antenna feeder (on the bottom-right corner) or a radial slot array on the ground plane (on the bottom-left corner). Two different geometries are considered for the PRS: a fishnet-like metasurface (on the top-left corner) and a dichroic annular strip-grating metasurface (on the top-right corner).

The possibility to generate TE-polarized focused beams, however, is important not only from a theoretical viewpoint but also from a practical one to mitigate dielectric losses [25]. Indeed, in wearable and implantable WPT applications [22], it is important to have focused fields with a negligible on-axis electric-field component so as to minimize the coupling with the very large dielectric losses exhibited by human tissues in the microwave and millimeter-wave ranges.

In this context, the authors investigated the possibility to realize a WPT link between TE-polarized BBLs in papers [1, 8]. While in paper [8] a *hybrid*-TE (HTE-) polarized Bessel beam has been obtained by means of a loop antenna excitation and an annular-strip grating metasurface, in paper [1] a *pure* TE-polarized Bessel beam has been theoretically excited through a radial slot array on the ground plane. In this paper, an effective and original theoretical analysis for the annular strip grating used in the HTE-polarized BBL is presented and corroborated through full-wave simulations on CST Microwave Studio [27]. Afterwards, the WPT performance of TE- and HTE-polarized BBLs is evaluated in terms of link budget, obtaining improved results with a purely TE-polarized BBL.

The paper is organized as follows: section "Design of TE-polarized BBLs" shows the theoretical leaky-wave approach needed to design a TE-polarized BBL. In section "Physical implementation," full-wave results of HTE- and TE-polarized BBLs are shown along with their physical implementation and the theoretical description of their metasurface and feeder. In section "Wireless power transfer," the WPT performance of the different resonant BBLs analyzed in this work are shown and compared. In particular, the transmission efficiency has been computed with an effective hybrid numerical and full-wave approach. Conclusions are finally drawn in section "Conclusion."

Design of TE-polarized BBLs

As mentioned in section "Introduction," resonant BBLs consist of a circular grounded dielectric slab enclosed by a metallic rim and with a PRS on top [19, 21] (see Figure 1). Purely TM(TE)-polarized BBLs can only be obtained by using ideal VED(VMD) sources, which generate a zeroth-order Bessel beam over the vertical electric(magnetic)-field component. Such beams maintain their transverse profile (thanks to the limited-diffraction property) up to the so-called *nondiffractive range* z_{ndr}, which is given by the following ray-optics approximation [2]:

$$z_{ndr} = \rho_{ap} \cot \theta_0, \tag{1}$$

where ρ_{ap} is the aperture radius, and θ_0 is the so-called *axicon angle* (measured with respect to the vertical z-axis). Resonant BBLs belong to the family of *leaky-wave* BBLs which possesses slightly different properties with respect to classical BBLs due to the intrinsic amplitude exponential decay on the aperture field distribution [28, 29].

https://doi.org/10.1017/S1759078723001538 Published online by Cambridge University Press

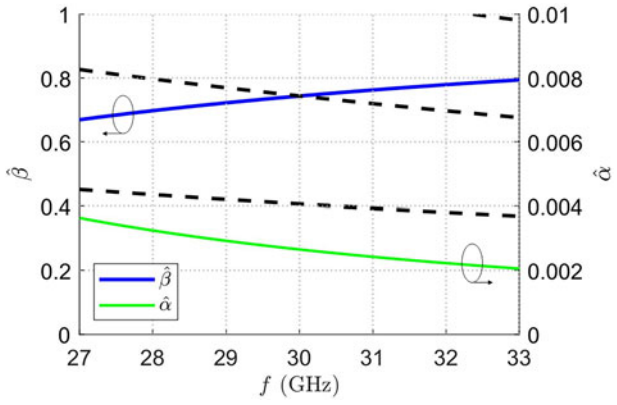

Figure 2. Dispersion curves of the normalized leaky-wave phase $\hat{\beta}$ (blue solid line) and attenuation $\hat{\alpha}$ (green solid line) constants vs. frequency *f*. The black dashed lines represent the dispersion curves of different radial resonances for TE-polarized BBLs.

In leaky-wave BBLs, the axicon angle θ_0 is related to the real part β of the complex, leaky, radial wavenumber $k_\rho = \beta - j\alpha$ [28]. While the attenuation constant α describes the power decay due to the radiation during the propagation inside the cavity, β, i.e., the leaky phase constant, is related to the axicon angle through the relation $\beta = k_0 \sin\theta_0$ (being k_0 the vacuum wavenumber).

In each polarization type, resonant BBLs generate the desired limited-diffractive beam through the interference of the outward cylindrical leaky wave coming from the source and the inward one given by the reflection on the circular metallic rim [20]. In particular, in order to enforce the correct constructive interference among such cylindrical waves, the outward and the inward contributions should add in phase and with almost the same amplitude. While the latter constraint is fulfilled by requiring a "small" value of the leakage constant α, the former has to be achieved by enforcing a correct radial resonance. From the boundary conditions, it follows that a resonance is achieved when the tangential electric field at the rim location is zero. In this regard, it is worthwhile noticing that depending on the polarization type, the tangential electric field will show a different aperture distribution, thus different design conditions have to be enforced for the TE and TM case. In particular, a null for the first or the zeroth-order of the first-kind Bessel function has to be placed on the circular metallic rim depending on the specific polarization [23]. As concerns the TE case, the following relation has to be verified [26]:

$$\beta\rho_{\text{ap}} = j_{1q}, \tag{2}$$

where j_{1q} is the qth null of the first-order Bessel function of the first kind.

As in paper [1], the choice of the working frequency, the aperture radius, and the number of nulls is fixed as follows: $f_0 = 30$ GHz, $\rho_{\text{ap}} = 15$ mm, and $q = 2$, respectively. At this point, the normalized leaky phase constant is fixed at $\hat{\beta} = \beta/k_0 \simeq 0.7436$ through equation (2). As concerns the normalized attenuation constant $\hat{\alpha} = \alpha/k_0$, it should be as low as possible in order to maintain almost the same amplitude between outward and inward cylindrical leaky waves [30]. A good design rule is to consider the inward wave power at the antenna rim equal to the 95% at least of the outward one at the antenna feeder which corresponds here to a normalized attenuation constant equal to $\hat{\alpha} = 0.0027$ as in papers [1, 9].

It is worth pointing out that a low value of α does not mean that the radiation efficiency of the proposed launcher is low. It is true that, in typical leaky-wave antennas (see, e.g., [31] and reference therein), the *radiation* efficiency η_r is often evaluated through the well-known expression $\eta_r = 1 - \exp(-2\alpha\rho_{\text{ap}})$. However, this formula ignores the cylindrical spreading factor that characterize cylindrical leaky waves, and assumes the structure to be terminated with an ideal absorber, whereas the leaky-wave launcher studied here is terminated over a circular metallic rim, which would make the radiation efficiency tend to one. This efficiency evaluation, however, does not take into account material losses, mismatching, and potential coupling of the source with other modes different from the dominant leaky wave. All these quantities could affect the *total* efficiency of the launcher. Since an air-filled cavity, a lossless dielectric and ideal metal are considered in the following, dielectric and ohmic losses are negligible. Therefore, the efficiency is not affected by material losses in our work (this assumption is totally reasonable in this frequency range [32]). The same holds for mismatching losses which are negligible (and not shown for brevity) since ideal sources have been assumed. The interesting point is related to the potential coupling with other existing modes (e.g., surface waves) that may subtract power to the leaky mode responsible for radiation. In this context, we properly designed the structure to avoid resonances with those modes (more details can be found in papers [19, 21]) and to limit the excitation of spurious modes that arise in HTE-polarized configurations, as shown next.

At this point, once the desired leaky wavenumber has been computed, it is necessary to suitably design the cavity to excite the targeted k_ρ value at f_0. To this aim, the design parameters available in a resonant BBL are the cavity height h and the equivalent PRS reactance X_s that can be computed through the methods described in paper [33]. The PRS is indeed typically realized through an isotropic metallic metasurface [34] which is represented by an imaginary scalar impedance $Z_s = jX_s$ since losses are negligible. This assumption is in general fully satisfactory for resonant BBLs [19–21]. Therefore, as shown in paper [1] and by following the analysis in papers [23, 33], the design parameters for the TE-polarized BBL analyzed in this work are fixed at: $h = 7.194$ mm and $X_s = 67.235\ \Omega$.

In order to verify the validity of the design, the transverse resonant technique [35] is applied on the transverse equivalent network (TEN) of the device, thus obtaining the relevant dispersion equation of the structure, as in papers [19, 20, 23]. In particular, the dispersion curve of the leaky mode can be found by solving the dispersion equation for the complex improper roots, using the Padé algorithm [36].

The results of this complex-mode analysis are reported in Figure 2. As shown, the dispersion curve of the leaky phase constant intersects the dispersive radial resonance at the working frequency f_0. Moreover, as concerns the dispersion curve of the leakage constant, very low values for $\hat{\alpha}$ are achieved around the working frequency, as desired in order to achieve the Bessel-beam distribution.

Once the theoretical design parameters are verified, it is necessary to implement from a practical viewpoint the excitation of the device and the PRS. These aspects are discussed in the following section "Physical implementation."

Physical implementation

In this section, we analyze the possibility to excite TE-polarized and HTE-polarized BBLs through two different feeders.

https://doi.org/10.1017/S1759078723001538 Published online by Cambridge University Press

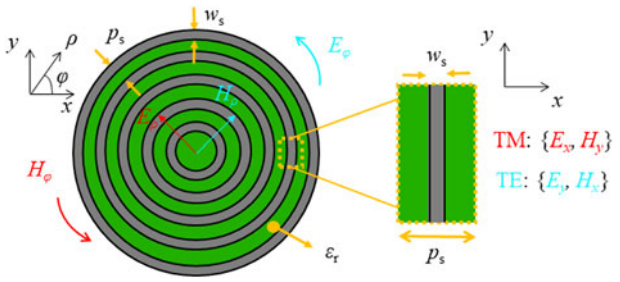

Figure 3. Pictorial representation of the proposed PRS composed by an annular strip grating with periodicity p_s and width w_s. The nonvanishing electromagnetic tangential field components in the case of an azimuthally symmetric device with a TE (light blue color) and TM (red color) are represented.

In particular, an effective theoretical analysis for the metasurface used here to enhance the TE components of a non-ideal TE excitation is presented.

Feeder

As discussed in section "Introduction," a purely TE-polarized BBL can only be obtained with an ideal VMD source. As shown in papers [8, 25, 26], loop antennas and feeding coils are not *ideal* VMD sources. Therefore, even if a well-designed TE-polarized resonant BBL is considered (as discussed in section "Design of TE-polarized BBLs"), the excitation through a simple loop feeder generates a hybrid-polarized field with a generally nonnegligible TM-field contribution (see Figure 4). This effect is due to the feeding point (with height $h_{\mathrm{lf}} \simeq \lambda_0/10$, being λ_0 the vacuum wavenumber at the working frequency f_0) of the loop antenna (with radius $R_{\mathrm{l}} \simeq \lambda_0/(2\pi)$) which breaks the azimuthal symmetry of the structure (see Figure 1). Therefore, a simple loop antenna does not excite a purely TE-polarized Bessel beam but rather an HTE one. However, as shown in paper [8], it is possible to reduce the undesired TM contributions by using an original homogenized metasurface consisting of an annular strip grating (see its pictorial representation on the top-right corner of Figure 1 and in Figure 3) whose innovative theoretical description and its dichroic behavior are presented in the following subsection "Metasurface."

As recently demonstrated in paper [1], an option to achieve the excitation of a purely TE-polarized Bessel beam is given by a radial slot array on the ground plane. In this work and in paper [1], the radial slots on the ground plane are ideally excited by dipole-like sources but, from a practical viewpoint, an ad hoc feeding scheme of the slots should be considered. The design and the optimization of the physical excitation of the slots will be addressed in future works.

Once the radial slot array on the ground plane is correctly excited, it represents the discrete counterpart of a continuous loop of radially directed magnetic surface current. The ideal, continuous source couples only with irrotational magnetic fields and, hence, it excites a pure, azimuthal symmetric, TE-polarized field. In this work and in paper [1], an array of $N = 8$ rectangular radial slots of width $w = 1$ mm and length $l = 2$ mm are considered with a uniform azimuthal distribution and a fixed radial distance from the vertical z-axis given by $R = 2.5$ mm (see Figure 1). It is worth pointing out that the slots have to be electrically small (please note that, in this work, $w = \lambda_0/10$ and $l = \lambda_0/5$), simultaneously excited with the same amplitude, and their number should

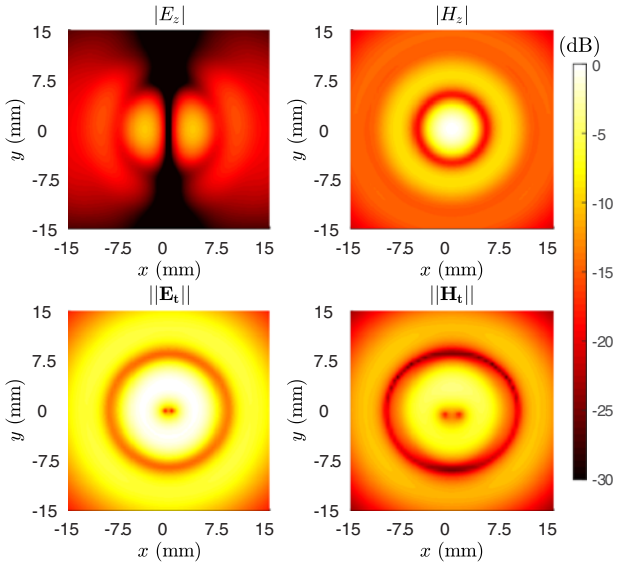

Figure 4. Full-wave results for the designed TE-polarized BBL with a typical fishnet-like metasurface as a PRS and a loop antenna near the ground plane as a feeder. All the components are normalized with respect to the maximum of their respective field on the $z = z_{\mathrm{ndr}}/2$ plane, where their absolute values are reported in dB.

be sufficiently high to well represent their continuous counterpart. The purity of the polarization is corroborated by the field envelope further reported in the analysis (see Figure 6): the E_z field component is indeed negligible with respect to the $||\mathbf{E}_t||$ contribution. Therefore, since a realistic pure TE excitation has recently been achieved in paper [1], it can be exploited to demonstrate and quantify the dichroic behavior of the annular strip grating proposed in paper [8].

Metasurface

The main difference between HTE-polarized and TE-polarized BBLs is given by their excitation scheme. In the former case, the hybrid character of the source call for radiating apertures able to enhance the TE field components with respect to the undesired TM ones.

As discussed in section "Design of TE-polarized BBLs," an inductive-like metasurface with $X_{\mathrm{s}} \simeq 67.235\ \Omega$ is needed in order to excite the desired leaky wavenumber and achieve the correct radial resonance at the working frequency $f_0 = 30$ GHz. A simple structure that allows for synthesizing a wide range of inductance values is the fishnet-like metasurface [30]. In particular, the desired X_{s} value is obtained by setting the distance among patches to $g = 0.86$ mm and the width of the metallic bridge among them to $w = 0.3$ mm, when the period is set to $p = 2$ mm (which is fully within the homogenization limit, viz. $p < \lambda_0/4$). Such a metasurface shows almost the same behavior for both TE and TM polarization [30] and thus is not well suitable for HTE-polarized BBLs that instead call for dichroic metasurfaces, such as the annular strip grating (see Figure 3).

An original approach is used here to theoretically describe the latter. As mentioned earlier, this kind of metasurface allows for enhancing the TE field components with respect to the TM ones. This effect clearly emerges from a direct comparison between the field envelopes in Figure 4, where a non-ideal TE source (the loop antenna) is used with a fishnet-like metasurface, and

https://doi.org/10.1017/S1759078723001538 Published online by Cambridge University Press

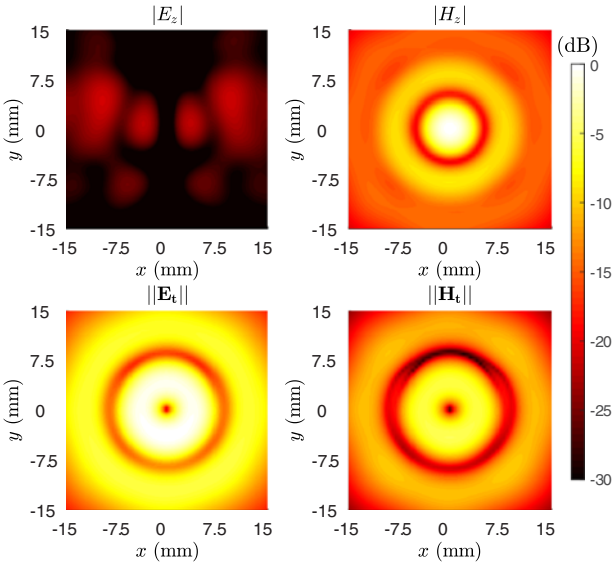

Figure 5. Full-wave results for the HTE-polarized BBL [8] obtained with a loop-antenna feeder and annular-strip-grating metasurface. All the components are normalized with respect to the maximum of their respective field on the $z = z_{\mathrm{ndr}}/2$ plane, where their absolute values are reported in dB.

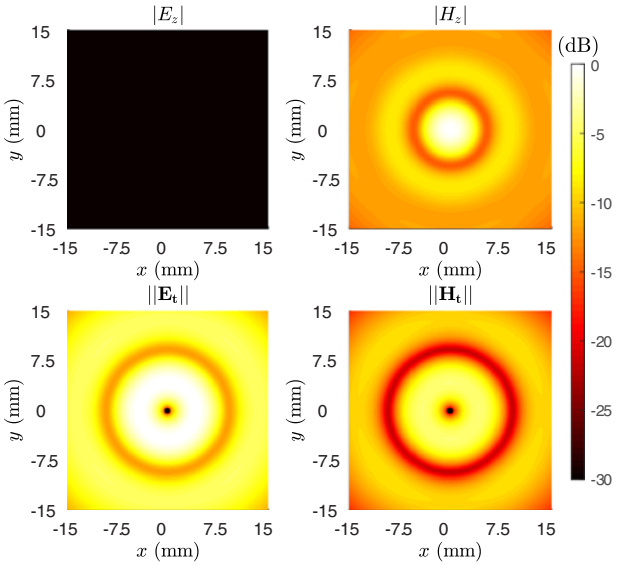

Figure 6. Full-wave results for the designed TE-polarized BBL proposed in paper [1]. In this case, a typical fishnet-like metasurface has been considered as PRS and a radial slot array on the ground plane as a feeder. All the components are normalized with respect to the maximum of their respective field on the $z = z_{\mathrm{ndr}}/2$ plane, where their absolute values are reported in dB.

that in Figure 5, where the same source is used with an annular strip grating. In the latter case, the E_z component is considerably reduced.

However, there is still a nonnegligible vertical component of the electric field that should be zero [23], even though its maximum value is much lower than the maximum value of $\mathbf{E}_t$. For this reason, we refer to both these cases as a HTE polarization and not as a purely TE-polarized Bessel beam as the one achieved with the radial-slot-array feeder and the typical fishnet-like metasurface (whose field distribution is reported in Figure 6).

The effect of the annular-strip-grating metasurface is strictly related to its *dichroic* nature. In order to understand this behavior, it is important to recall that the only nonvanishing contributions for the TE and the TM polarizations are H_z, H_ρ, E_ϕ, and E_z, E_ρ, H_ϕ, respectively [23]. As shown in Figure 3, the only tangential components on the PRS are $H_\rho(E_\rho)$ and $E_\phi(H_\phi)$ for the TE(TM) polarization. Therefore, the tangential electric-field components in the TE(TM) case are locally parallel(perpendicular) to the metallic strips, thus revealing the dichroic nature of the metasurface which shows an inductive (capacitive) behavior in the TE(TM) case. Moreover, by virtue of the azimuthal symmetry of the structure, we can consider a section at constant ϕ and consider a local linear approximation of annular strip grating to treat it as a conventional metal strip grating [37] (see Figure 3). Since the period of the unit cell is much smaller than the wavelength (viz., $p \ll \lambda_0$), we can also exploit the homogenization principle and characterize the whole metasurface by studying the scattering properties of the zeroth-order Floquet harmonic under TE and TM incidence. As for more conventional homogenized metasurfaces, the annular strip grating admits a simple surface-impedance representation: an inductive one for the TE case and a capacitive one for the TM case. These impedance values can in principle be found using either approximate analytical formulas [37] or conventional full-wave approaches [30].

However, it is worthwhile to note that such PRS has to be printed on some thin dielectric substrates placed on the BBL top

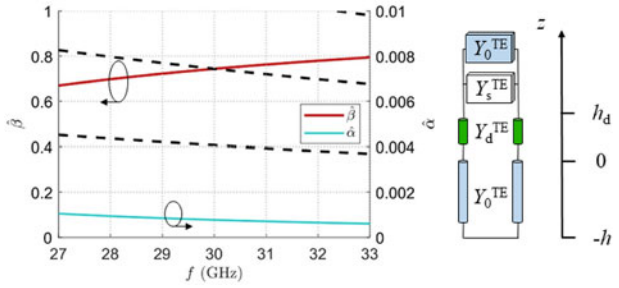

Figure 7. The TEN for the TE-polarized contribution in the resonant BBL with the annular strip grating as PRS is represented along with its dispersive diagram.

with negligible losses, height h_{d} and relative dielectric constant ε_{r}. Therefore, a more precise TEN has to be considered in order to correctly enforce the radial resonance at the desired working frequency f_0. As shown in Figure 7, the TEN is given by two cascaded transmission lines: one of length h with the characteristic admittance of the TE mode in the air Y_0 and one of length h_{d} with the characteristic admittance of the TE mode in the dielectric Y_{d}. The metasurface and the air medium are represented by their equivalent admittances $Y_{\mathrm{s}}^{\mathrm{TE}} = -j/X_{\mathrm{s}}^{\mathrm{TE}}$ and Y_0, respectively.

After numerical optimization, it is found that the desired resonance at f_0 is obtained for an annular strip grating with parameters $p_{\mathrm{s}} = \lambda/10$ and width $w_{\mathrm{s}} = 0.26$ mm printed on a lossless dielectric with $\varepsilon_{\mathrm{r}} = 3$ and thickness $h_{\mathrm{d}} = 0.127$ mm, as shown in Figure 7. It is worth mentioning that this choice of parameters leads to $X_s^{\mathrm{TE}} = 35.18\ \Omega$, which considerably differs from the value reported at the beginning of subsection "Metasurface"; this is a consequence of the phase shift introduced by the thin dielectric layer considered here.

However, if loop-antenna feeders are considered, nonnegligible TM components are excited and need to be taken into account. For this purpose, we analyzed the behavior of the annular strip grating under TM polarization and found

https://doi.org/10.1017/S1759078723001538 Published online by Cambridge University Press

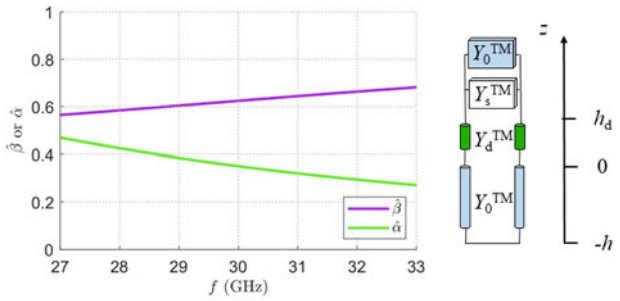

Figure 8. The TEN for the TM-polarized contribution in the resonant BBL with the annular strip grating as PRS is represented along with its dispersive diagram.

$X_s^{TM} = -5530.66\ \Omega$. As opposed to the TE case, the surface impedance in the TM case is large in absolute value and negative. As a result, while the PRS is rather reflective for the TE case, it is almost *transparent* for the TM case, thus strongly promoting the efficient radiation of TE leaky waves with respect to TM leaky waves. This statement is corroborated by the dispersive diagram reported in Figure 8 for the TM case along with the TEN of the TM wave (the meaning of each admittance is the same of the TE case but for the TM polarization). As shown, the TM leakage constant $\hat{\alpha}$ is very high (due to the very low reflectivity of the PRS for this polarization), thus a TM-polarized Bessel beam can no longer be effectively generated by this leaky mode (because the reflected inward cylindrical leaky wave would be significantly damped, thus a stationary aperture field would not be efficiently created).

The surface impedance models of the annular strip metasurface, its dichroic nature, and the related dispersive properties of the leaky modes supported in the BBLs can be verified by considering a purely TE (as the radial slot array proposed in paper [1]) and a purely TM (a coaxial cable [23]) excitation scheme.

In the former case, a comparison between the results achieved through the realistic metasurface and its surface impedance model $X_s = X_s^{TE}$ has been considered in Figure 9(a), where the H_z field radial profile (normalized to its maximum) at $z = z_{ndr}/2$ is reported. (All TE field components have been evaluated, but not shown for brevity; similar agreement is obtained in all cases). The analysis of the dual case is shown in Figure 9(b). The impressive agreement between the realistic metasurface and the surface impedance model with an ideal source corroborate the theoretical analysis of the proposed metasurface: the same field distribution has indeed been achieved with the theoretical X_s value and the annular strip grating for both polarizations.

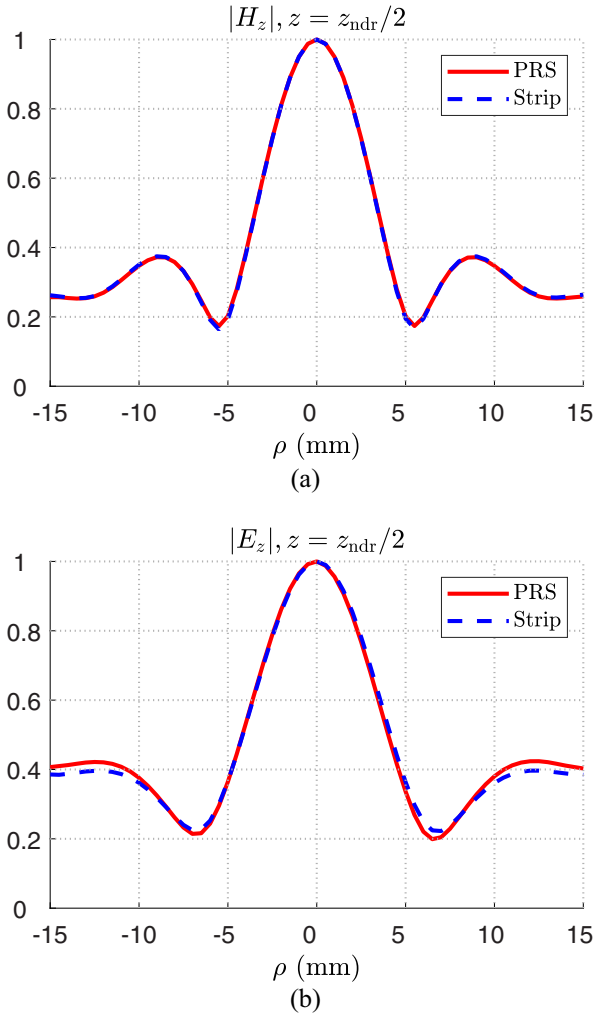

Figure 9. Full-wave validation of the theoretical description of the PRS when a purely (a) TE- or (b) TM-polarized source are considered inside the resonant BBL designed in section "Design of TE-polarized BBLs." The blue dashed lines represent the normalized (a) H_z and the (b) E_z field components with respect to their maximum at $z = z_{ndr}/2$ when the annular strip grating is considered as PRS. The red solid lines report the same field components when the PRS is implemented by a surface impedance boundary condition with (a) $Z_s = jX_s^{TE}$ or (b) $Z_s = jX_s^{TM}$.

Wireless power transfer

After conducting a thorough characterization of the HTE-polarized BBL, it is interesting to evaluate its performance in terms of WPT. The intrinsic high-focusing capabilities, together with the system compactness, make BBLs valuable candidates to be exploited within these types of applications. As shown in papers [8–10], by placing two identical launchers one in front of the other, it is possible to create limited-diffractive WPT links. Here, we focus specifically on the launchers that were created using the specifications provided in Section II.

When using two BBLs within a wireless link, the calculation of power budget becomes a crucial aspect, taking advantage of their unique propagation properties within the *nondiffractive range*. While in previous works the evaluation of the WPT efficiency has been achieved through an accurate, analytical, and numerical approach based on the equivalence theorem in the spatial [38] and spectral [39] domains, a fast, straightforward, yet effective method has been considered in this work. In particular, the general-purpose link budget model given in paper [40] is used to produce an estimation of the power budget of the presented WPT scenario when two BBLs are used as the transmitting (TX) and receiving (RX) antennas [1]. In order to facilitate the comparison of obtained performance, the two BBLs are chosen of the same polarization. The Norton equivalent circuit of a rectenna can be exploited to rigorously estimate the received power [40]:

$$P_r = (1/8)|I_{eq}|^2/\mathrm{Re}\left[Y_a(\omega)\right], \tag{3}$$

where $Y_a(\omega)$ is the internal complex admittance of the considered antenna, i.e., the HTE-polarized BBLs. As can be inferred from equation (3), the correct computation of I_{eq} allows for safely estimating the overall link power budget. According to the numerical algorithm [40], the electromagnetic field components of the TX

https://doi.org/10.1017/S1759078723001538 Published online by Cambridge University Press

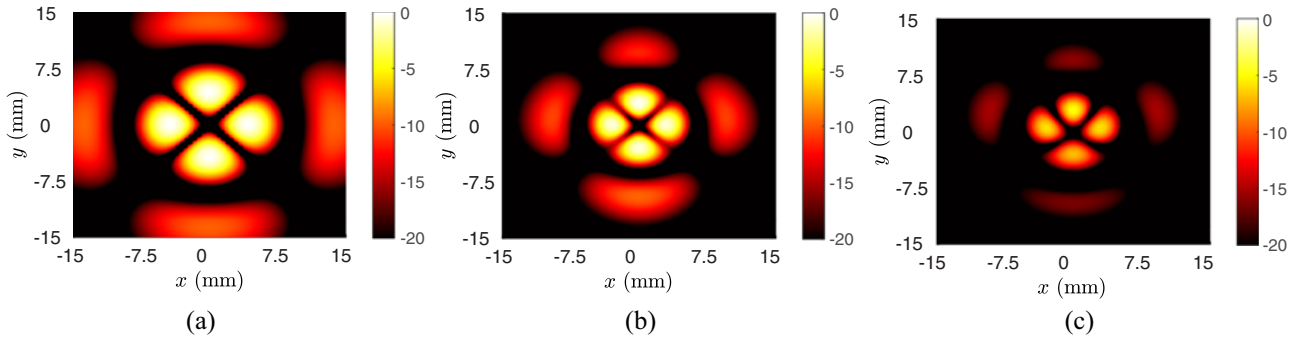

Figure 10. Computed equivalent current density for the (a) TE-polarized BBL [1] and two HTE-polarized BBLs achieved through a loop antenna feeder, and (b) an annular strip grating [8], or (c) a fishnet-like metasurface. All the plots are evaluated on a *xy*-plane at $z = 10$ mm and reported in a dB scale after the normalization with respect to the maximum among them.

Table 1. Received power for BB launchers with different feeders, metasurfaces, and polarizations

TX-RX distance (mm)	P_r (dBm) TE [1]	P_r (dBm) HTE Annular strip grating	P_r (dBm) HTE Fishnet metasurface
20	9.8	6.6	2.6
30	3.2	1.2	−4.3
40	−1.1	−2.4	−7.6

and RX launchers are replaced by the equivalent electric and magnetic surface currents computed on a plane positioned between the two launchers, and the current I_{eq} is then precisely determined by solving the surface integral of the following expression [40]:

$$\hat{\boldsymbol{n}} \cdot [\mathbf{E}_i(P_S) \times \mathbf{H}_R(P_S) - \mathbf{E}_R(P_S) \times \mathbf{H}_i(P_S)] \quad (4)$$

where P_S are the points belonging to the interposed surface S between the TX and the RX, with unit vector $\hat{n}$, whereas $\mathbf{E}_i$, $\mathbf{H}_i$, $\mathbf{E}_R$, and $\mathbf{H}_R$ are the electric and magnetic fields of the TX and RX launchers, respectively.

The fields $\mathbf{E}_i$ and $\mathbf{H}_i$ are computed and extracted by the full-wave characterization of a single launcher radiating in free space, acting as the TX, whereas $\mathbf{E}_R$ and $\mathbf{H}_R$ refer to the receiver and are numerically evaluated, reducing remarkably the global computational time required for a full-wave simulation of the studied WPT link.

Figure 10(a) shows the computed equivalent current density for a link made of two pure TE-polarized BBLs (fed with radial slot arrays) [1], whereas Figure 10(b) and (c) refer to the equivalent current density evaluated for the HTE-polarized BBLs (fed with loop antenna) designed with an annular strip grating and a fishnet-like metasurface, respectively. Both cases are computed and plotted for a reference distance of $z = 10$ mm. As can be noticed, they both present four main lobes in which the overall equivalent current density is mainly concentrated. However, the pure TE-polarized case exhibits higher peaks that reflects in a higher receiver power, as is further addressed in the following results.

The receiver power levels for the analyzed WPT links are computed for three different TX-RX operating distances, namely 20, 30, and 40 mm. The link performances are listed in Table 1 and the comparison is carried out for the three different polarization types. The obtained values are computed considering an input power at the TX side equal to 21 dBm.

As can be inferred from Table 1, when a pair of pure TE-polarized BBLs is considered, the received power levels are higher than both cases with an HTE polarization due to the higher polarization purity and the correct excitation of the desired dominant leaky mode. It is worth pointing out that the HTE-polarized WPT link performance is greater when a dichroic metasurface is considered rather than a typical isotropic one (such as the fishnet-like metasurface). This effect is related to the promising ability of the innovative strip-grating metasurface to enhance the TE field components with respect to the TM ones when the device is excited with a *non-ideal* VDM source. Therefore, since the BBL parameters are chosen in order to excite a TE-polarized Bessel beam, the WPT efficiency is higher as the TE polarization purity increases.

Conclusion

In this work, it is shown how a TE-polarized Bessel-beam is excited by a leaky-wave resonant cavity with a radial slot array on the ground plane. As expected from a theoretical viewpoint, a dominant zeroth-order Bessel beam over the vertical magnetic field component H_z and a negligible vertical electric field E_z have been achieved. This innovative radial slot array and a more conventional coaxial cable are then respectively used as ideal TE and TM sources to corroborate the theoretical analysis of an innovative dichroic metasurface under TE and TM polarization, respectively. This kind of metasurface is very useful when a non-ideal source, such as a loop antenna, is considered and the device is designed to resonate with a TE polarization. Finally, the link power budget is evaluated for different cases obtaining interesting results with respect to the state-of-the-art and showing a higher power transmission efficiency as the polarization purity increases.

Supplementary material. The supplementary material for this article can be found at https://doi.org/10.1017/S1759078723001538.

Acknowledgements. This work was funded by the Italian Ministry of Education, University and Research (MIUR) within the framework of the PRIN 2017-WPT4WID ("Wireless Power Transfer for Wearable and Implantable Devices") ongoing project.

Competing interests. The authors declare none.

References

1. **Negri E, Benassi F, Fuscaldo W, Masotti D, Burghignoli P, Costanzo A and Galli A** (2022) Effective TE-polarized Bessel-beam excitation for

wireless power transfer near-field links. In *52nd European Microwave Conference (EuMC 2022)*, Milan, IT, 1–4.
2. **Durnin J** (1987) Exact solutions for nondiffracting beams. I. The scalar theory. *Journal of the Optical Society of America A* **4**(4), 651–654.
3. **Hernández-Figueroa HE, Zamboni-Rached M and Recami E** (2007) *Localized Waves*. Hoboken, NJ: John Wiley & Sons.
4. **Hernández-Figueroa HE, Zamboni-Rached M and Recami E** (2013) *Nondiffracting Waves*. Weinheim: John Wiley & Sons.
5. **McGloin D and Dholakia K** (2005) Bessel beams: Diffraction in a new light. *Contemporary Physics* **46**(1), 15–28.
6. **Pimenta RCM, Soriano G, Paschaloudis KD, Ettorre M, Zerrad M and Amra C** (2023) Power transfer efficiency for obstructed wireless links using Bessel beams. *Optics Express* **31**(22), 35493–35506.
7. **Negri E, Fuscaldo W, Burghignoli P and Galli A** (2023) Leaky-wave analysis of TM-, TE-, and hybrid-polarized aperture-fed Bessel-beam launchers for wireless power transfer links. *IEEE Transactions on Antennas and Propagation* **71**(2), 1424–1436.
8. **Benassi F, Fuscaldo W, Negri E, Paolini G, Augello E, Masotti D, Burghignoli P, Galli A and Costanzo A** (2022) Comparison between hybrid- and TM-polarized Bessel-beam launchers for wireless power transfer in the radiative near-field at millimeter waves. In *51st European Microwave Conference (EuMC 2021)*, London„ 1–4.
9. **Benassi F, Fuscaldo W, Masotti D, Galli A and Costanzo A** (2021) Wireless power transfer in the radiative near-field through resonant Bessel-beam launchers at millimeter waves. In *2021 IEEE Wireless Power Transfer Conference (WPTC)*, San Diego, CA, USA, 1–4.
10. **Heebl JD, Ettorre M and Grbic A** (2016) Wireless links in the radiative near field via Bessel beams. *Physical Review Applied* **6**(3), 034018.
11. **Paković S, Zhou S, González-Ovejero D, Pavone SC, Grbic A and Ettorre M** (2021) Bessel–Gauss beam launchers for wireless power transfer. *IEEE Open Journal of Antennas and Propagation* **2**, 654–663.
12. **Negri E, Benassi F, Fuscaldo W, Masotti D, Burghignoli P, Costanzo A and Galli A** (2023) Recent advances in beam focusing through resonant Bessel-beam launchers for millimeter-wave WPT applications. In *17th European Conference on Antennas and Propagation (EuCAP 2023)*, Florence, Italy, 1–4.
13. **Negri E, Del Biondo L, Fuscaldo W, Burghignoli P and Galli A** (2023) Wireless radiative near-field links through wideband Bessel-beam launchers. In *53rd Europ. Microw. Conf. (EuMC 2023)*, Berlin, Germany 1–4.
14. **Ettorre M, Pavone SC, Casaletti M, Albani M, Mazzinghi A and Freni A** (2018) Near-field focusing by non-diffracting Bessel beams. In Boriskin Artem and Sauleau Ronan (eds), *Aperture Antennas for Millimeter and Sub-Millimeter Wave Applications*. Cham: Springer,243–288.
15. **Comite D, Fuscaldo W, Podilchak SK, Hílario-Re PD, Gómez-Guillamón Buendía V, Burghignoli P, Baccarelli P and Galli A** (2018) Radially periodic leaky-wave antenna for Bessel beam generation over a wide-frequency range. *IEEE Transactions on Antennas and Propagation* **66**(6), 2828–2843.
16. **Pavone SC, Ettorre M, Casaletti M and Albani M** (2016) Transverse circular-polarized Bessel beam generation by inward cylindrical aperture distribution. *Optics Express* **24**(10), 11103–11111.
17. **Pavone SC, Ettorre M, Casaletti M and Albani M** (2021) Analysis and design of bessel beam launchers: Transverse polarization. *IEEE Transactions on Antennas and Propagation* **69**(8), 5175–5180.
18. **Pavone SC, Ettorre M and Albani M** (2016) Analysis and design of Bessel beam launchers: Longitudinal polarization. *IEEE Transactions on Antennas and Propagation* **64**(6), 2311–2318.
19. **Fuscaldo W, Valerio G, Galli A, Sauleau R, Grbic A and Ettorre M** (2016) Higher-order leaky-mode Bessel-beam launcher. *IEEE Transactions on Antennas and Propagation* **64**(3), 904–913.
20. **Ettorre M and Grbic A** (2012) Generation of propagating Bessel beams using leaky-wave modes. *IEEE Transactions on Antennas and Propagation* **60**(8), 3605–3613.
21. **Negri E, Fuscaldo W, Ettorre M, Burghignoli P and Galli A** (2022) Analysis of resonant Bessel-beam launchers based on isotropic metasurfaces. In *16th European Conference on Antennas and Propagation (EuCAP 2022)*, Madrid, Spain, 1–4.
22. **Costanzo A, Apollonio F, Baccarelli P, Barbiroli M, Benassi F, Bozzi M, Burghignoli P, Campi T, Cruciani S, di Meo S, Feliziani M, Fuscaldo W, Galli A, Liberti M, Maradei F, Marracino P, Masotti D, Paolini G, Pasian M, Perregrini L, Schettini G and Silvestri L** (2021) Wireless power transfer for wearable and implantable devices: A review focusing on the wpt4wid research project of national relevance. In *2021 XXXIV General Assembly and Scientific Symposium of the International Union of Radio Science (URSI GASS)*, Rome, IT, 1–4.
23. **Negri E, Fuscaldo W, Burghignoli P and Galli A** (2022) A leaky-wave analysis of resonant bessel-beam launchers: Design criteria, practical examples, and potential applications at microwave and millimeter-wave frequencies. *Micromachines* **13**(12), 2230.
24. **Ettorre M, Rudolph SM and Grbic A** (2012) Generation of propagating Bessel beams using leaky-wave modes: Experimental validation. *IEEE Transactions on Antennas and Propagation* **60**(6), 2645–2653.
25. **Lu P, Bréard A, Huillery J, Yang X-S and Voyer D** (2018) Feeding coils design for TE-polarized Bessel antenna to generate rotationally symmetric magnetic field distribution. *IEEE Antennas and Wireless Propagation Letters* **17**(12), 2424–2428.
26. **Lu P, Voyer D, Bréard A, Huillery J, Allard B, Lin-Shi X and Yang X-S** (2017) Design of TE-polarized Bessel antenna in microwave range using leaky-wave modes. *IEEE Transactions on Antennas and Propagation* **66**(1), 32–41.
27. CST products Dassault Systèmes, France (2022). http://www.cst.com
28. **Fuscaldo W, Comite D, Boesso A, Baccarelli P, Burghignoli P and Galli A** (2018) Focusing leaky waves: a class of electromagnetic localized waves with complex spectra. *Physical Review Applied* **9**(5), 054005.
29. **Fuscaldo W, Benedetti A, Comite D, Baccarelli P, Burghignoli P and Galli A** (2020) Bessel-Gauss beams through leaky waves: Focusing and diffractive properties. *Physical Review Applied* **13**(6), 064040.
30. **Fuscaldo W, Tofani S, Zografopoulos DC, Baccarelli P, Burghignoli P, Beccherelli R and Galli A** (2018) Systematic design of THz leaky-wave antennas based on homogenized metasurfaces. *IEEE Transactions on Antennas and Propagation* **66**(3), 1169–1178.
31. **Galli A, Baccarelli P and Burghignoli P** (2016) Leaky-wave antennas. In Webster JG (ed), *Wiley Encyclopedia of Electrical and Electronics Engineering*. Hoboken, NJ: Wiley, 1–20.
32. **Fuscaldo W** (2019) Rigorous evaluation of losses in uniform leaky-wave antennas. *IEEE Transactions on Antennas and Propagation* **68**(2), 643–655.
33. **Fuscaldo W, Galli A and Jackson DR** (2022) Optimization of 1-D unidirectional leaky-wave antennas based on partially reflecting surfaces. *IEEE Transactions on Antennas and Propagation* **70**(9), 7853–7868.
34. **Burghignoli P, Fuscaldo W and Galli A** (2021) Fabry–Perot cavity antennas: the leaky-wave perspective. *IEEE Antennas and Propagation Magazine* **63**(4), 116–145.
35. **Sorrentino R and Mongiardo M** (2005) *Transverse Resonance Techniques*. John Wiley & Sons, Ltd.
36. **Galdi V and Pinto IM** (2000) A simple algorithm for accurate location of leaky-wave poles for grounded inhomogeneous dielectric slabs. *Microwave and Optical Technology Letters* **24**(2), 135–140.
37. **Luukkonen O, Simovski C, Granet G, Goussetis G, Lioubtchenko D, Raisanen AV and Tretyakov SA** (2008) Simple and accurate analytical model of planar grids and high-impedance surfaces comprising metal strips or patches. *IEEE Transactions on Antennas and Propagation* **56**(6), 1624–1632.
38. **Borgiotti G** (1966) Maximum power transfer between two planar apertures in the Fresnel zone. *IEEE Transactions on Antennas and Propagation* **14**(2), 158–163.
39. **Pavone SC and Albani M** (2019) Design of a wireless link at microwaves in the radiative near-field by using RLSA Bessel beam launchers. In *2019 PhotonIcs & Electromagnetics Research Symposium-Spring (PIERS-Spring)*. Rome, Italy: IEEE, 289–294.
40. **Rizzoli V, Masotti D, Arbizzani N and Costanzo A** (2010) CAD procedure for predicting the energy received by wireless scavenging systems in the near- and far-field regions. In *2010 IEEE MTT-S International Microwave Symposium*, Anaheim, CA, USA, 1768–1771.

https://doi.org/10.1017/S1759078723001538 Published online by Cambridge University Press

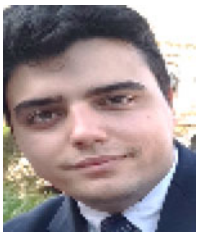

Edoardo Negri was born in Orvieto, Italy, in 1997. He received the B.Sc. and M.Sc. degrees (cum laude) in electronic engineering, with honorable mention for the academic curriculum, from Sapienza University of Rome, Rome, Italy, in July 2019 and 2021, respectively, where he is currently pursuing the Ph.D. degree in Information and Communications Technologies (applied electromagnetics curriculum). From March to May 2023, Mr. Negri has been a visiting PhD student in the Institut d'Électronique et de Télécommunications de Rennes (IETR), Université de Rennes 1, Rennes, France. His main research interests are leaky waves, metasurfaces, focusing devices, and wireless power transfer at high frequencies (ranging from microwaves to terahertz). Mr. Negri received the "Antonio Ventura" Award as one of the best engineering students at the Sapienza University of Rome in 2022, the IEEE Antennas and Propagation Society (APS) Fellowship Award in 2023, and the European Microwave Association (EuMA) Internship Award in 2023.

Francesca Benassi received the Ph.D. degree (*cum laude*) in Electronics, Telecommunications and Information Technologies Engineering from the University of Bologna, Bologna, Italy, in 2022. She is currently working as junior assistant professor at the Department of Electrical, Electronic and Information Engineering (DEI) "Guglielmo Marconi." Her main research interests involve the design of wearable rectennas for Wireless Power Transfer applications both at microwave and at millimeter waves. Dr. Benassi has been awarded with the MTT-S Graduate Fellowship Award and the EuMA Internship Award in 2021.

Walter Fuscaldo received the B.Sc. and the M.Sc. (*cum laude*) degrees in Telecommunications Engineering from Sapienza University of Rome, Rome, Italy, in 2010 and 2013, respectively. In 2017, he received the Ph.D. degree (*cum laude* and with the Doctor Europaeus label) in Information and Communication Technology (applied electromagnetics curriculum) from both the Department of Information Engineering, Electronics and Telecommunications (DIET) and the Institut d'Électronique et de Télécommunications de Rennes (IETR), Université de Rennes 1, Rennes, France, under a cotutelle agreement between the institutions. In 2014, 2017, and 2018, he was a Visiting Researcher and in 2023 a Visiting Scientist with the NATO-STO Center for Maritime Research and Experimentation, La Spezia, Italy. In 2016, he was a Visiting Researcher with the University of Houston, Houston, TX, USA. Since July 2017, he was a Postdoc Researcher at Sapienza University of Rome, and since July 2020, he joined the Institute for Microelectronics and Microsystems (IMM), Rome, Italy, as a Researcher of the National Research Council of Italy. His current research interests include propagation of leaky waves, surface waves and plasmonic waves, analysis and design of leaky-wave antennas, generation of localized electromagnetic waves, graphene electromagnetics, metasurfaces, and THz spectroscopy and antennas. Dr. Fuscaldo was awarded several prizes, among which are the prestigious Young Engineer Prize for the Best Paper presented at the 46th European Microwave Conference in 2016 and the Best Paper in Electromagnetics and Antenna Theory at the 12th European Conference on Antennas and Propagation in 2018. He is currently an Associate Editor of the *IET Microwaves, Antennas and Propagation* journal and *IET Electronic Letters*.

Diego Masotti (M'00, SM'16) received the Ph.D. degree in electric engineering from the University of Bologna, Italy, in 1997. In 1998, he joined the University of Bologna where he now serves as an Associate Professor of electromagnetic fields. From 2021, he has the role of coordinator of the Telecommunications Engineering Master Degree course. His research interests are in the areas of nonlinear microwave circuit simulation and design, with emphasis on nonlinear/electromagnetic co-design of integrated radiating subsystems/systems for wireless power transfer and energy harvesting applications. He authored more than 70 scientific publications on peer-reviewed international journals and more than 140 scientific publications on proceedings of international conferences. Dr. Masotti serves in the Editorial Board of Electronic Letters, of the Hindawi journal of Wireless Power Transfer, of IEEE Access, and is a member of the Paper Review Board of the main Journals of the microwave sector.

Paolo Burghignoli was born in Rome, Italy, in 1973. He received the Laurea degree (cum laude) in Electronic Engineering and the Ph.D. degree in Applied Electromagnetics from Sapienza University of Rome, Rome, Italy, in 1997 and 2001, respectively. In 1997, he joined the Department of Electronic Engineering, Sapienza University of Rome, where he is currently an Associate Professor with the Department of Information Engineering, Electronics and Telecommunications. He has authored about 250 articles in international journals, books, and conference proceedings. He is a co-author of the book *Electromagnetic Shielding: Theory and Applications* (Wiley-IEEE Press, 2023, 2nd ed.). His research interests include the analysis and design of planar antennas and arrays, leakage phenomena in uniform and periodic structures, numerical methods for integral equations and periodic structures, propagation and radiation in metamaterials, electromagnetic shielding, transient electromagnetics, and graphene electromagnetics. He is currently serving as an Associate Editor of the *IET Electronics Letters* and the *International Journal of Antennas and Propagation* (Hindawi).

Alessandra Costanzo is Full Professor of Electromagnetic Fields at the University of Bologna, Campus of Cesena, since September 2018. She carries out her research in the field of the CAD of RF and microwave circuits and systems such as: Multiple-input-Multiple Output (MIMO), UWB systems, radio frequency identification systems (RFID), and "rectenne" (multi-band rectifying antennas) for the collection of RF energy, specialized for wearable applications. This activity is carried out through the development of innovative project procedures based on the combination of electromagnetic theory, numerical simulation, and nonlinear analysis based on the harmonic balancing method. She studies and develops systems for wireless power transmission (WPT) adopting both near-field and far-field techniques for different operating frequencies and different power levels. She has developed innovative solutions in the field of non-invasive structural monitoring, exploiting electromagnetic interference, and reverse-modeling of antenna arrays.

https://doi.org/10.1017/S1759078723001538 Published online by Cambridge University Press

Alessandro Galli received the Laurea degree in Electronic Engineering and the PhD degree in Applied Electromagnetics from Sapienza University of Rome, Italy. Since 1990, he has been with the Department of Information Engineering, Electronics and Telecommunications of the same university. In 2000, he became an Assistant Professor and in 2002 an Associate Professor in the sector of Electromagnetic Fields; in 2012, he passed the National Scientific Qualification and then definitively achieved the role of Full Professor in the same sector and university. He authored about 300 papers in indexed journals, books, and conference proceedings. His research interests include theoretical and applied electromagnetics, mainly focused on modeling, numerical analysis, and design of antennas and passive devices from microwaves to terahertz. His research activities also concern the areas of geoelectromagnetics, bioelectromagnetics, and plasma heating. Dr. Galli was the Italian representative of the Board of Directors of the European Microwave Association (EuMA) from 2010 to 2015. He was the recipient of various grants and prizes for his research activity; in 2017, he was elected as the "Best Teacher" of the European School of Antennas (ESoA).

https://doi.org/10.1017/S1759078723001538 Published online by Cambridge University Press